Supplementary information:

A folded viral noncoding RNA blocks host cell exoribonucleases through programmed remodeling of RNA structure

Authors: Anna-Lena Steckelberg, Benjamin M. Akiyama, David A. Costantino, Tim L. Sit, Jay C. Nix, Jeffrey S. Kieft

SI Materials and Methods

DNA templates and mutagenesis

DNA templates for *in vitro* transcription were gBlocks ordered from IDT, cloned into pUC19 and verified by sequencing. Mutations were introduced by site-directed mutagenesis and verified by sequencing. RNA constructs for Xrn1 degradation assays contained the xrRNA sequence plus 30 nucleotides of the endogenous upstream sequence ('leader sequence') to allow loading of the exoribonucleases. CRSV xrRNA constructs contained the RCNMV leader sequence because secondary structures in the endogenous CRSV sequence prevented 5′-exoribonuclease loading. Numbering throughout the manuscript is in reference to the crystallized RNA construct.

Below are sequences of the dianthoviral 3′UTRs as used in Xrn1 degradation assays with the T7 promoter underlined, the leader sequence in italics and minimal xrRNA highlighted in bold. Transcription with T7 RNA polymerase was started with 3 guanosine nucleotides (shown in lower case, not part of the endogenous viral sequence) for enhanced transcription efficiency.

RCNMV
TAATACGACTCACTATAggg*AACACTTTCATACTTGGTTAATTGGTTCTTTTAA***GCGTAGCCTCCACCCGA**
GTTGCAAGAGGGGAACGCGCAGTCTCGCCGACCCTGTTGGCAAACAGTAAAATTGCAAAAAATAG
AGTGCTAGGAGTAGTTCCCGTACCCGCGGGAGCAAGACCCTACTACAGTAGACGAACCGGCATCGGA
CCCTGGGAAACAGGTACCTAGCGTATTAATAGGTCGCTAGAAATCGGGCGGGCTTCACCTTCGGGTA
ACCCGCCGTCGAGAGGGAAAACCTCTGTGTGGTTGTGCGCACGTCGTTGTCGGAAGACTCTCACTGTT
GTAGTTATTTCCTTTTTCTTTTAGGTAGGAGCACTTGCTCAGAGGGCGCATACCTCTGGTAAAACAAA
ATTGGCCCCTGAGAGTAGAAAACTCAGGTTAATAAAACAGGAGAATATTTACCTAGTCGTATAACGG
CTAGGTACCCC

SCNMV
TAATACGACTCACTATAggg*TCGAAGCCGTCGAACGCCTATGTATTTGGTTAATGCAA***GCGTAACCTCCAT**
CCGAGTTGCAAGAGAGGGAAACGCAGTCTCGCCGACCCTGTTGCCAAACAGTAAAATTGGAAAAA
ATAGAGTGTTAGGAGTAGTTCCCGTACCCGCGGGACAAGAACCTATTGTAGTAGACGAACCGGTCTC
GGACCCTGGTAAACAGGTACCTAGCGTAATAGAAGGTCGCTAGAAATCGGGTGGGCTTCACCTACGG
GTAACCCACCGTCGAGAGGGAAAACCTCTGTGTGGTTGTGCGCACGTCGTTTCCTGAAGAATCTCACT
GCAGTAGTTATTTCCTTTTCCTTTTAGGCTAGAAGCACTTGCTACGGAGGGCGCATACCTTCGGTTAAA
CAAAATTGGCCCCTGAGAGTAGAAAACTCAGGTTAATAAAACAGGAGATTATTTGCTTAGTCGTATA
ACGGCTAAGCACCCC

CRSV (with RCNMV leader sequence)
TAATACGACTCACTATAggg*AACACTTTCATACTTGGTTAATTGGTTCTTTTAA***CCGTAGCCGCCAACAAA**
GTTGCAAGAGCGGGCGTTGCTAGCCTTTGCCGACCCTGCTTCCTGGCGCAGCAAATCCAGAGAAA
AACAGAGTGTTAGGATGTTGTCTTCTTACCTTAGGAGACGAGAACCTACGAGGCACAAGTCAGTGAT
CCGGATCCTGAGAAACAGGCAGTCCGCAACCTTAGTAGGGGGCGGCAGACGGGTGGGCTTCAGCCTT
GGGGTGGTACCCAAGGATAACCTGCCGACGTGGTGGAGACACCAGGCGTGTTGTGGCGTCATCGAAT
CACGAACACTTGTGTTGGCCGTAGTTAAATTCGTGTCAGTCCTTTTCTTTTGTTTGTATGTGGGGTCAG

TGTGCGTCACACGCACCGACGGGAGTAGAAAACCCGCCGTCAAGTAAAAACAGGGAAACGAACACC
GGTGGGTATAACCCCCGGGCCCCT

***In vitro* transcription**

DNA templates for *in vitro* transcription were amplified by PCR using custom DNA primers and Phusion Hot Start polymerase (New England BioLabs). 2.5 mL transcription reactions were assembled using 1000 µL PCR reactions as template (~0.2 µM template DNA), 6 mM each NTP, 60 mM $MgCl_2$, 30 mM Tris pH 8.0, 10 mM DTT, 0.1% spermidine, 0.1% Triton X-100, T7 RNA polymerase and 2 µL RNasin RNase inhibitor (Promega) and incubated overnight at 37°C. After inorganic pyrophosphates were precipitated by centrifugation, the reactions were ethanol precipitated and purified on a 7 M urea 8% denaturing polyacrylamide gel. RNAs of the correct size were gel-excised, eluted overnight at 4°C into ~40 mL of diethylpyrocarbonate (DEPC)-treated milli-Q filtered water (Millipore) and concentrated using Amicon Ultra spin concentrators (Millipore).

Protein expression and purification

The expression vector for *Kleuveromyces lactis* Xrn1 (1) (residues 1-1245) and *Kleuveromyces lactis* Dxo1 (2) were gifts of Prof. Liang Tong at Columbia University, the expression vector for *Bacillus subtilis* RNase J1 (3) was a gift of Ciaran Condon at CNRS, and the expression vector for *Bdellovibrio bacteriovorus* RppH (4) was a gift of Joel Belasco at NYU. All recombinant proteins were 6XHis-tagged, expressed in *E. coli* BL21 cells and purified using Ni-NTA resin (Thermo), followed by size exclusion with either a Superdex 75 or Superdex 200 column in an AKTA pure FPLC (GE Healthcare). The final product was stored in buffer containing 20 mM Tris pH 7.3, 300 mM NaCl, 1 mM DTT or 2 mM BME, and 10% glycerol (1 mM EDTA was added to the RNase J1 sample) at -80°C. The purity of the recombinant proteins was verified by SDS-PAGE and Coomassie staining.

5′-3′ exoribonuclease degradation assay

4 µg RNA was resuspended in 40 µL 100 mM NaCl, 10 mM $MgCl_2$, 50 mM Tris pH 7.5, 1 mM DTT and re-folded at 90°C for 3 minutes then 20°C for 5 minutes. 3 µL recombinant RppH (0.5 µg/µL stock) was added and the samples were split into two 20 µL reactions (-/+ exoribonuclease). 1 µL of the recombinant Xrn1 (0.8 µg/µL stock) was added where indicated. All reactions were incubated for 2 hrs (or the indicated time) at 30°C using a thermocycler. The degradation reactions were resolved on a 7 M urea 10% denaturing polyacrylamide gel and stained with ethidium bromide.

RNA degradation assays using other 5′→3′ exoribonucleases were performed as described above, using 10 µL of recombinant Dxo1 (0.6 µg/µL) or 4 µL of recombinant RNase J1 (0.5 µg/µL) per 2 µg RNA.

^{32}P-3′-end labelling of RNA and quantitative Xrn1 degradation assay

In order to quantitate Xrn1 resistance activity, RNAs were radiolabeled at their 3′ terminus. To this end, Cytidine-3′-monophosphate (Cp) was 5′-end labeled with [γ32-P]ATP (PerkinElmer) using T4 polynucleotide kinase (PNK). This was done in a 10 µL labeling reaction that contained 5 µL of 5 mCi [γ32-P]ATP, 0.2 mM Cp, 1 µL T4 PNK (New England BioLabs) and 1 µL 10x PNK buffer, and incubated at 37ºC for 90 minutes followed by heat-inactivation at 65ºC for 15 minutes. 1 µL of the 5′-end-labeled ^{32}PCp was ligated to the 3′ end of 20 µg of the desired RNA construct using T4 RNA ligase (Fermentas) for 12 hrs at 16ºC (10 µL ligation reaction: 20 µg RNA, 1 µL ^{32}PCp, 1 µL T4 RNA ligase buffer, 2 µL T4 RNA ligase). ^{32}P-labeled RNA was purified using Micro-Bio P-30 spin columns (Bio-Rad) according to the manufacturer's instructions. Counts per minute (cpm) were determined using a Bioscan QC-4000 XER radiation counter (Hyland Scientific).

15000 cpm ^{32}P-labeled RNA was used in 10 µL Xrn1 degradation assays as described above, with degradation products resolved by 7 M urea 10% polyacrylamide gel electrophoresis and visualized using a phosphor screen and Typhoon 9400 scanner (GE Life Sciences). Xrn1 resistance was defined as the percentage of Xrn1-resistant degradation products (resistant RNA) relative to the total amount of untreated RNA (input RNA). Quantitation was performed using ImageQuant LAS 4000 (GE Healthcare) software.

Reverse transcription of Xrn1 degradation products and mapping of the Xrn1 stop site

To determine the Xrn1 stop site at single-nucleotide resolution, 50 µg *in vitro* transcribed RNA was degraded using recombinant RppH and Xrn1 as described above (the reaction volume was scaled up to 400 µL, and 20 µL of each enzyme was used). The degradation reaction was resolved on a 7 M urea 8% polyacrylamide gel, then the Xrn1-

resistant degradation product was cut from the gel and purified using 25:24:1 Phenol:Chloroform:Isoamyl alcohol extraction (Fisher) according to manufacturer's instructions. Once recovered, the RNA was reverse transcribed using Superscript III reverse transcriptase (Thermo) and a FAM (6-fluorescein amidite)-labeled sequence-specific reverse primer (IDT) with an $(A)_{20}$-stretch at the 5′ end to allow cDNA purification with oligo(dT) beads. 10 µL RT reactions contained 1.2 pM RNA, 0.25 µL of 0.25 µM FAM-labeled reverse primer, 1 µL 5x First-Strand buffer, 0.25 µL of 0.1 M DTT, 0.4 µL of 10 mM dNTP mix, 0.1 µL Superscript III reverse transcriptase (200 U/µL) and were incubated for 1 hour at 50°C. To hydrolyze the RNA template after reverse transcription, 5 µL of 0.4 M NaOH was added and the reaction mix incubated at 90°C for 3 min, followed by cooling on ice for 3 min. The reaction was neutralized by adding 5 µL of acid quench mix (1.4 M NaCl, 0.57 M HCl, 1.3 M sodium acetate pH 5.2), then 1.5 µL oligo(dT) beads (Poly(A)Purist MAG Kit (Thermo)) were added and the cDNA purified on a magnetic stand according to the manufacturer's instructions. The cDNA was eluted in 11 µL ROX-HiDi and analyzed on a 3500 Genetic Analyzer (Applied Biosystems) for capillary electrophoresis. A Sanger sequencing (ddNTP) ladder of the undigested RNA was analyzed alongside the degradation product as reference for band annotation.

Mutagenesis of RCNMV infectious clone and viral infection

Mutations were introduced into an infectious cDNA construct of RCNMV RNA-1 (5) using the QuikChange II Site-Directed Mutagenesis Kit (Agilent Technologies). Primer pairs are listed in the table below. Mutation reactions were transformed into DH5-alpha chemically competent *E. coli* (New England BioLabs) and plasmid DNA was purified using the ZymoPURE™ Plasmid Miniprep Kit (Zymo Research). Plasmid DNAs were linearized with *Sma*I (New England BioLabs) prior to *in vitro* transcription with the MEGAscript™ T7 Transcription Kit (Thermo) according to the supplier's instructions. 1 µL of mutant and/or wild-type RCNMV RNA-1 transcript was combined with an equal volume of wild-type RCNMV RNA-2 transcripts in 100 µL sodium phosphate buffer, pH 7.2 for plant inoculations. Carborundum-dusted leaves of *Nicotiana benthamiana* (2 leaves/plant x 2 plants/construct) were rub inoculated with RCNMV transcripts and the infection allowed to proceed for 3 days. Total RNA was extracted from inoculated leaves (100 mg) using TRIzol™ (Thermo) and Direct-zol™ kits (Zymo Research). Briefly, leaf tissue was frozen in liquid N_2 prior to disruption with glass beads. TRIzol was added to the pulverized tissue and the RNA was extracted according to the Direct-zol™ instructions. Total RNA was resuspended in 50 µL dH_2O.

Oligonucleotides used for mutagenesis:

Name	Sequence[1]
A3464T	GGTTCTTTTAAGCGT**T**GCCTCCACCCGAGTTGC
A3464TRC	GCAACTCGGGTGGAGGC**A**ACGCTTAAAAGAACC
PKmut	CAAGAGGGGAACGCGCAGT**TCT**GCCGACCCTGTTGGCAAAC
PKmutRC	GTTTGCCAACAGGGTCGGC**AGA**ACTGCGCGTTCCCCTCTTG
PKcomp	TTAAGCGTAGCCTCCACCC**AGA**TTGCAAGAGGGGAACGCGCAGT**TCT**GCCG ACCCTGTTGGCAAACAG
PKcompRC	CTGTTTGCCAACAGGGTCGGC**AGA**ACTGCGCGTTCCCCTCTTGCAA**TCT**GGG TGGAGGCTACGCTTAA

[1]Mutated nucleotide(s) in bold typeface.

Northern blotting

1 µg of total RNA from mock- or RCNMV-infected cells was resuspended in 2x formamide RNA loading buffer and run on a 6% denaturing PAGE gel (Invitrogen) with an RNA ladder (Thermo). Gels were stained with ethidium bromide and imaged to obtain the position of the RNA ladder. The RNA from the gels was subsequently transferred to a HyBond-N+ nylon membrane (GE Life Sciences) using an electrophoretic transfer apparatus (Idea Scientific). The membrane was crosslinked using a UV Stratalinker (VWR) at 120 mJ and blocked at 42°C using ULTRAhyb Oligo hybridization and blocking buffer (Thermo) for 2 hours while rotating. Blots were probed rotating overnight at 42°C with a 35-mer DNA oligo prepared as described below and washed four times in 2x saline-sodium citrate (SSC) buffer with 0.5% SDS for 10 minutes at 42°C. The blots were imaged using a phosphor screen and Typhoon 9400 scanner (GE Life Sciences) and were aligned with the ethidium bromide-stained image of the gels to obtain the position of size standards from the RNA ladder.

Preparation of probes for Northern blots

DNA oligos used as Northern probes were ordered from IDT (RCNMV 5′-GAGACTGCGTGTTCCCCTCTTGCAACTCGGGTGGAGGC-3′ and 5.8S rRNA 5′-CGTGCCCTCGGCCTAATGGC-3′). 100 pmol of DNA was incubated with 2 µL 5 mCi [γ32-P]ATP (PerkinElmer) and 4 µL T4 PNK (New England BioLabs) in a 100 µL reaction for 2 hours at 37°C and purified using Micro-Bio P-30 spin columns (Bio-Rad). The radiolabeled probe was heated to 100°C for 2 minutes and resuspended in 10 mL of ULTRAhyb Oligo hybridization buffer (Thermo). Blots were incubated with 10 mL of the resuspended probe overnight at 42°C.

RNA crystallization and diffraction data collection

RNA for crystallization was prepared as described above. The sequence used for *in vitro* transcription was 5′-ggCGTAACCTCCATCCGAGTTGCAAGAGAGGGAAACGCAGTCTCGGGCGGCATGGTCCCAGCCTCCTCGCTGGCGCCGCCTGGGCAACATGCTTCGGCATGGCGAATGGGACC-3′ where the underlined sequence belongs to the hepatitis delta ribozyme (6) that was used to generate homogenous 3′ ends. Two extra guanosine nucleotides were added to the 5′ end of the sequence for enhanced transcription efficiency (shown as lowercase letters). Ribozyme cleavage was induced at the end of transcription reaction by adding $MgCl_2$ (final conc. 120 mM) and incubating for 10 min at 65°C. Ribozyme-cleaved RNA was purified on a 7 M urea 8% polyacrylamide gel as described above. 5 mg/mL RNA was re-folded at 65°C for 3 minutes in a buffer containing 30 mM HEPES pH 7.5, 20 mM $MgCl_2$, and 100 mM KCl. Crystal Screens I and II, Natrix I and II, and the Nucleic Acid Mini Screen (all from Hampton Research) were used to perform initial screens at 20°C with sitting-drop vapor diffusion crystallization. Initial hits were optimized using custom screens. The RNAs used for the final structural analysis were crystallized in 50 mM sodium cacodylate trihydrate pH 6.5, 0.2 M potassium chloride, 0.1 M magnesium acetate tetrahydrate, 14% w/v PEG 8000. Crystals were buffer-exchanged into freezing solution (mother liquor containing 20% ethylene glycol and 20 mM Iridium (III) hexammine to obtain derived crystals for phasing) and flash-frozen in liquid nitrogen for x-ray diffraction. Diffraction data were collected at Advanced Light Source Beamline 4.2.2 using ‘shutterless’ collection at the Iridium L-III edge (1.0972 Å) at 100°K. 180° datasets were collected with 0.2° oscillation images. Data were indexed, integrated, and scaled using XDS (7).

Structure determination and refinement

The data were collected and processed to 2.55 Å, but only data to 3.0 Å were used for phasing. Nine Iridium (III) hexammine sites were identified and used in SAD phasing within the AutoSol function of Phenix (overall FOM = 0.5) (8). The map was used to build an initial model, which was improved through iterative rounds of model building and refinement (simulated annealing, Rigid-body, B-factor refinement) using COOT (9, 10) and Phenix (8). Only data to 2.9 Å were used for refinement. The final model contains all 45 nucleotides. Crystal diffraction data, phasing, and refinement statistics are contained in Table S1.

RNA and DNA labeling for smFRET

Fluorescently labeled RNAs for smFRET were prepared as described (11). In brief, Cy5-labeled RNA 5′ fragments were ligated to unlabeled RNA 3′ fragments. RNA 5′ fragments harboring reactive amine modifications (Dharmacon) and a 5′-monophosphate were labeled with monoreactive Cy5 (GE Life Sciences) and purified by reverse-phase HPLC. RNA 3′ fragments were transcribed using T7 RNA polymerase and purified by denaturing polyacrylamide gel electrophoresis as described above. 3′ fragments were then treated with recombinant BdRppH for 2 hours at 37°C in 1X EC3 buffer (50 mM Tris-HCl pH 7.5, 100 mM NaCl, 10 mM $MgCl_2$) and 1 mM DTT followed by 25:24:1 Phenol:Chloroform:Isoamyl alcohol extraction and ethanol precipitation to convert the 5′-triphosphorylated RNA to 5′-monophosphorylated RNA (to allow ligation by T4 DNA ligase). Fluorescently labeled 5′ fragments and RppH-treated 3′ fragments were assembled by DNA-splinted RNA ligation using T4 DNA ligase and purified by denaturing polyacrylamide gel electrophoresis.

A 5′ biotin-labeled DNA oligo harboring a reactive amine modification (5′-biotin-TTACTGTTTGGCAACAG(iAmMC6T)**GT-3′, IDT) was labeled with monoreactive Cy3 (GE Life Sciences) and purified by reverse-phase HPLC.

Labeled 5′-SCNMV WT

5′P-GUUAAUGCAAGCGUAACCUCCA(5-N-U)*CCGAGUUGCAAGAGA-3′

Labeled 5′-SCNMV $P1_{EXT}$
5′P-GUUAAUGCAACGAGACUGCGUAACCUCCA(5-N-U)*CCGAGUUGCAAGAGA-3′

3′-SCNMV WT
5′-GGGAAACGCAGTCTCGCCGACACTGTTGCCAAACAGT-3′

3′-SCNMV PK_{S2}
5′-GGGAAACGCAGT**TCTA**CCGACACTGTTGCCAAACAGT-3′

DNA oligo for splinted ligation
5′-GAGACTGCGTTTCCCTCTCTTGCAACTCGG-3′

* 5-N-U = 5-Aminoallyl-uridine
**iAmMC6T = Internal Amino Modifier C6 dT

Single-molecule FRET
Cy5-labeled purified RNAs were annealed to biotinylated Cy3-labeled DNA oligo and immobilized on PEGylated cover slides (Ted Pella, Inc.). PEGylated cover slides were prepared as described (12). Slides were imaged on a total internal reflection fluorescence microscope (Nikon Eclipse Ti-E) using an Andor iXon+ DU897 CCD camera with a 100 msec integration time. The image was split using the DV2 Dualview (Photometrics) and custom Semrock filters. FRET studies were performed in 100 mM NaCl, 10 mM $MgCl_2$, 50 mM Tris pH 7.5, 10% glycerol, 0.1 mg/mL BSA, 2 mM Trolox, 1% glucose, 1 mg/mL catalase, and 1 mg/mL glucose oxidase. Analysis was performed using custom MATLAB (Release 2017a, The MathWorks) scripts.

Supplementary Figures and Legends

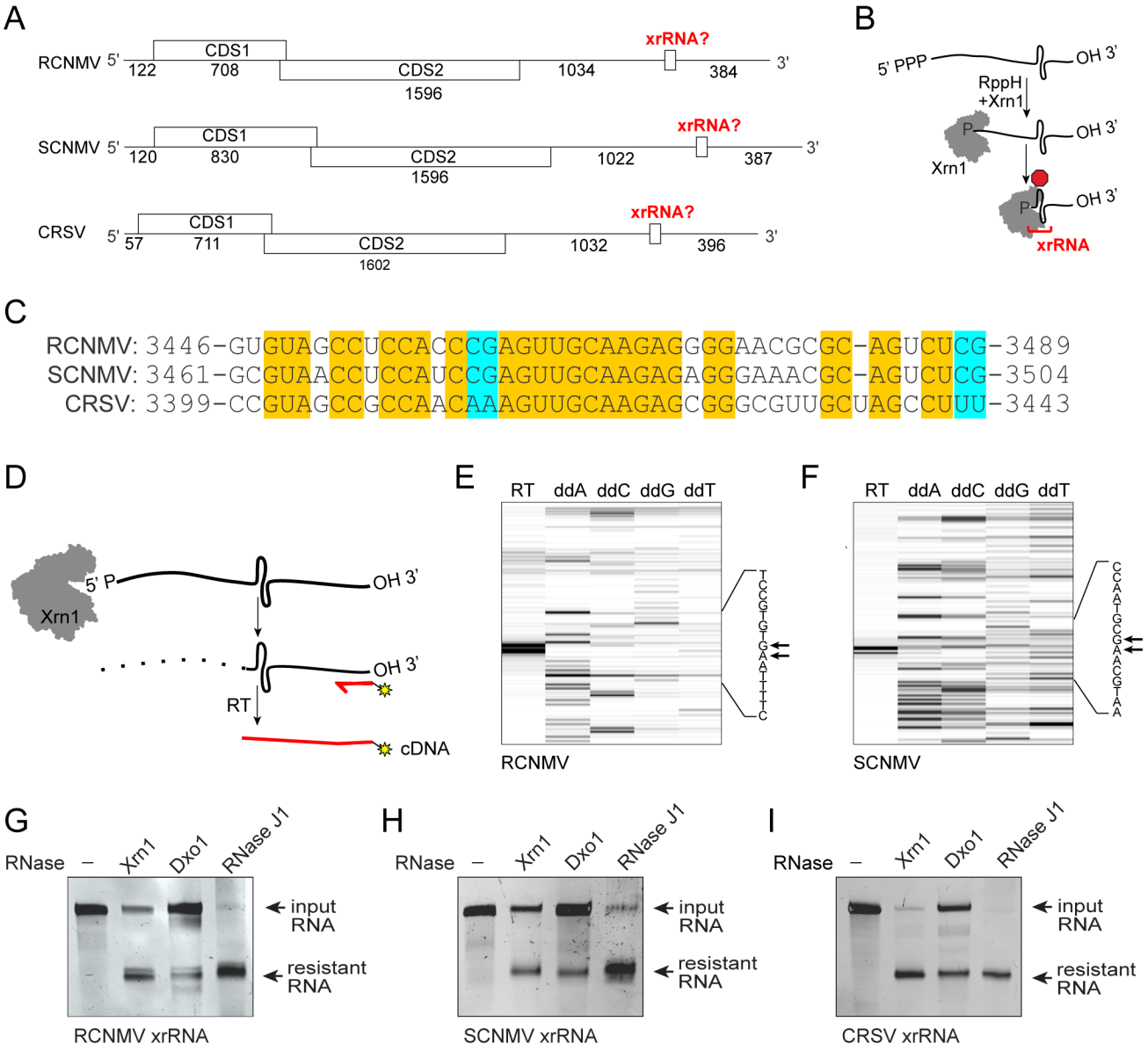

Fig. S1. Dianthovirus xrRNA is a robust general roadblock against 5′→3′ exoribonucleolytic decay. (*A*) Schematic of dianthovirus RNA1, with location of putative xrRNAs in red and open reading frames shown. Nucleotide length of different parts is included. (*B*) Scheme of *in vitro* Xrn1 degradation assay. (*C*) Alignment of the minimal Xrn1-resistant RNA sequence from RCNMV, SCNMV and CRSV. Conserved nucleotides are highlighted in yellow, co-varying nucleotides in cyan. (*D*) Schematic representation of the reverse transcription (RT) reaction of Xrn1 degradation products used to identify the Xrn1 stop site. cDNA was transcribed using a FAM-labeled reverse primer. (*E, F*) Capillary electrophoresis of cDNA from Xrn1 degradation reactions of RNA containing the RCNMV (*E*) or SCNMV (*F*) xrRNA sequence. Dideoxy sequencing lanes are labeled and used to determine the sequence around the Xrn1 stop site. Arrows depict the Xrn1 stop site. (*G-I*) xrRNA from RCNMV (*G*), SCNMV (*H*), or CRSV (*I*) was incubated in the presence of recombinant RppH and the indicated 5′-3′ exoribonucleases, and the degradation products were resolved by denaturing PAGE and visualized by ethidium bromide staining.

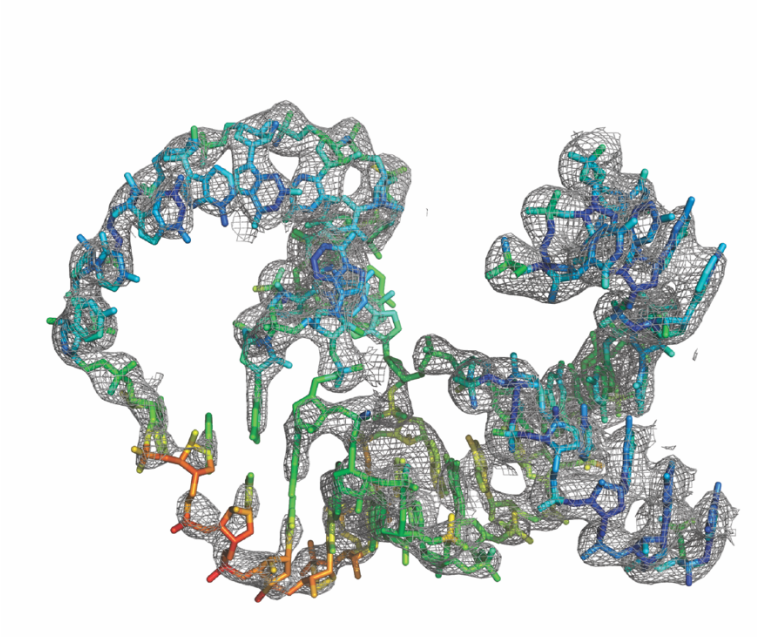

Fig. S2. Representative electron density. Final $2F_o$-F_c electron density map after model building and refinement (grey mesh, 1.5σ contour level) superimposed on the final model. Colors represent b-factors (red denotes highest B factors, blue lowest).

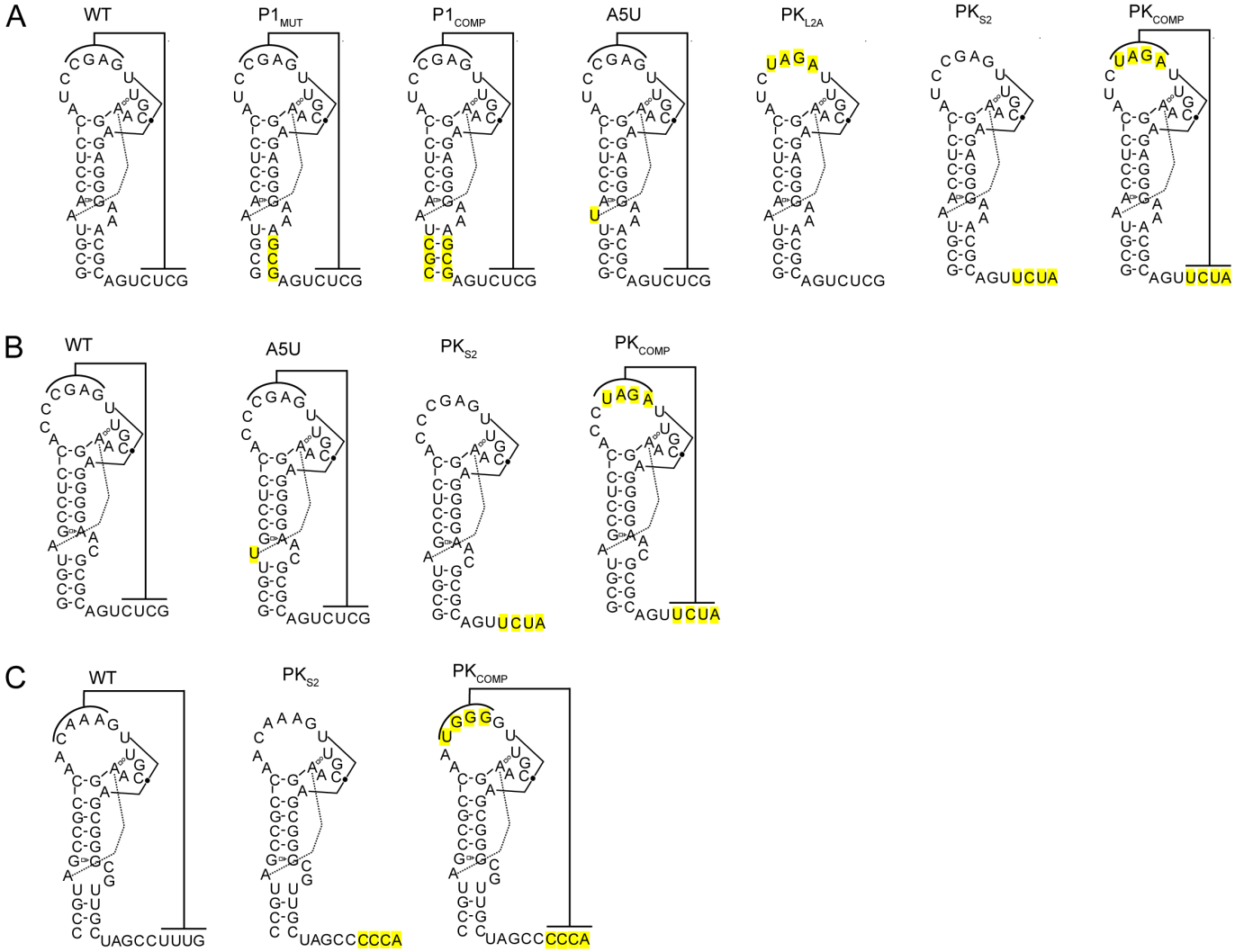

Fig. S3. Diagrams of mutants used in functional assays. (*A*) Secondary structures of WT and mutant SCNMV xrRNA constructs used in *in vitro* assays. (*B*) Proposed secondary structures of WT and mutant RCNMV xrRNA constructs used in *in vitro* assays and viral infection. (*C*) Proposed secondary structures of WT and mutant CRSV xrRNA constructs used in *in vitro* assays. For substitution mutants, yellow highlights indicate the location of the mutation. For all RNAs, the sequence shown was preceded by a 30 nucleotide-long leader known to allow efficient loading of Xrn1.

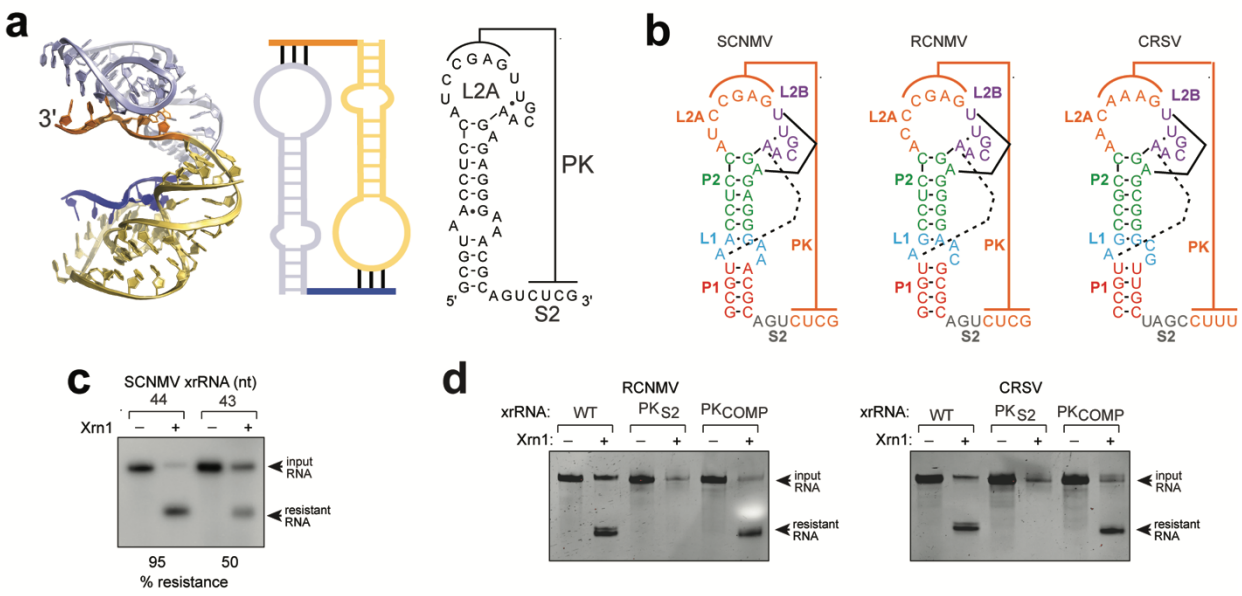

Fig. S4. Conserved pseudoknot interactions in Dianthovirus xrRNAs. (*A*) Left: ribbon diagram of two adjacent crystallized RNA molecules. 3' ends involved in intermolecular base pairing are shown in orange and blue. Middle: Scheme of crystallographic dimer, colors match diagram on left. Right: Alternate conformation with base pairs formed *in cis*. (*B*) Secondary structure diagram of crystallized SCNMV xrRNA (left) and of proposed secondary structures of RCNMV xrRNA (middle) and CRSV xrRNA (right). The putative PK is shown in orange. Diagrams include a nucleotide on the 3′ end that was not present in the crystallized RNA but increases Xrn1 resistance (see panel (*C*)). (*C*) *In vitro* Xrn1 degradation assay of RNA containing the crystallized SCNMV xrRNA element (43) or a 1 nt 3'-extended xrRNA (44). SCNMV xrRNA (44) shows increased Xrn1 resistance, presumably through a more stable PK. (*D*) Xrn1 degradation assay of *in vitro* transcribed RCNMV (left) and CRSV (right) xrRNA. Xrn1 degradation products were resolved by denaturing PAGE and visualized by ethidium bromide staining. Mutants are analogous to SCNMV mutation PK_{S2} and PK_{COMP} (Fig. S3).

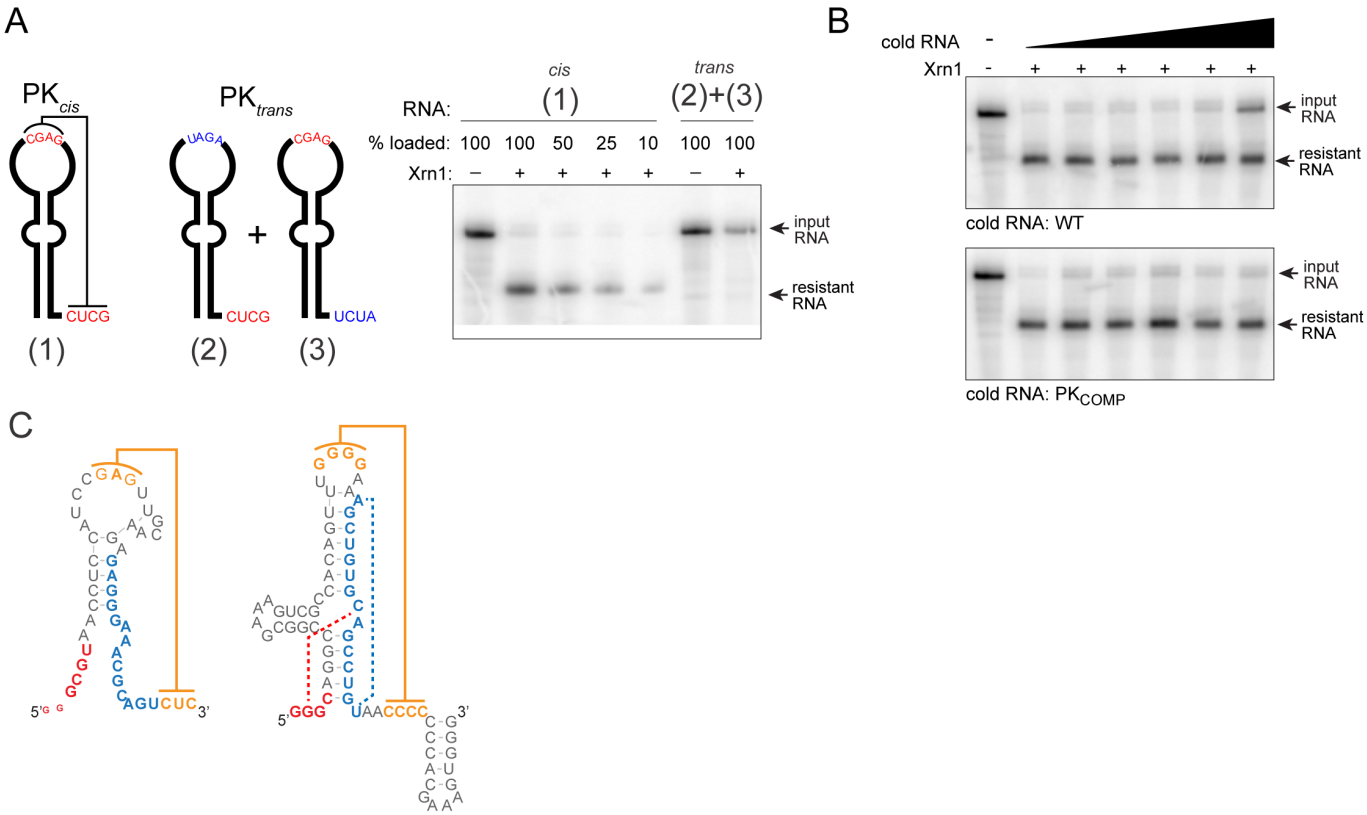

Fig. S5. The PK does not function *in trans* (as a dimer). (*A*) Left: RNA used for *in vitro* Xrn1 degradation assay. PK$_{cis}$ xrRNA can form the L2A-S2 interaction *in cis* and *in trans,* while PK$_{trans}$ can only form the L2A-S2 interaction *in trans.* Right: Autoradiograph of ^{32}P-labeled Xrn1 degradation products, note that the PK$_{trans}$ construct does not provide Xrn1 resistance. (*B*) Xrn1 degradation of ^{32}P-labeled SCNMV xrRNA in the presence of increasing amounts of cold SCNMV xrRNA (WT or PK$_{COMP}$). Xrn1 resistance is not concentration-dependent, arguing against formation of the PK interaction *in trans.* (*C*) Secondary structure diagram of modeled SCNMV xrRNA PK conformation (left) and ZIKV xrRNA1 (right). Colors match those in Fig. 3.

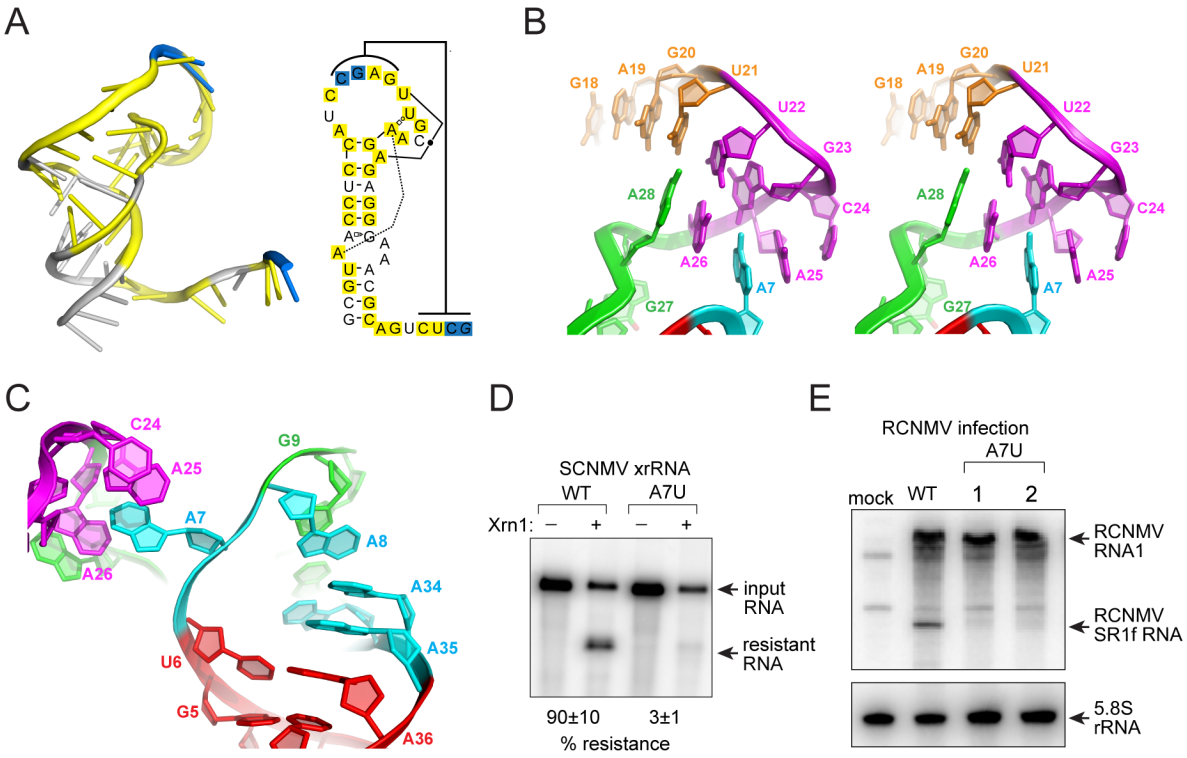

Fig. S6. Important determinants of dianthovirus xrRNA function. (*A*) Ribbon representation (left) and secondary structure diagram (right) of SCNMV xrRNA. Conserved nucleotides are shown in yellow, co-varied nucleotides are in blue. (*B*) Stereo image of the L2B-A7 stacking interaction. (*C*) Details of the L2B-A7 interaction. (*D*) *In vitro* Xrn1 degradation assay on ^{32}P-3′-end-labeled xrRNA WT and A7U mutant. Average % resistance from 3 individual experiments (-/+ SD). (*E*) Northern blot of total RNA from mock- or RCNMV-infected *N. benthamiana.* Probe against RCNMV 3′UTR or 5.8S rRNA.

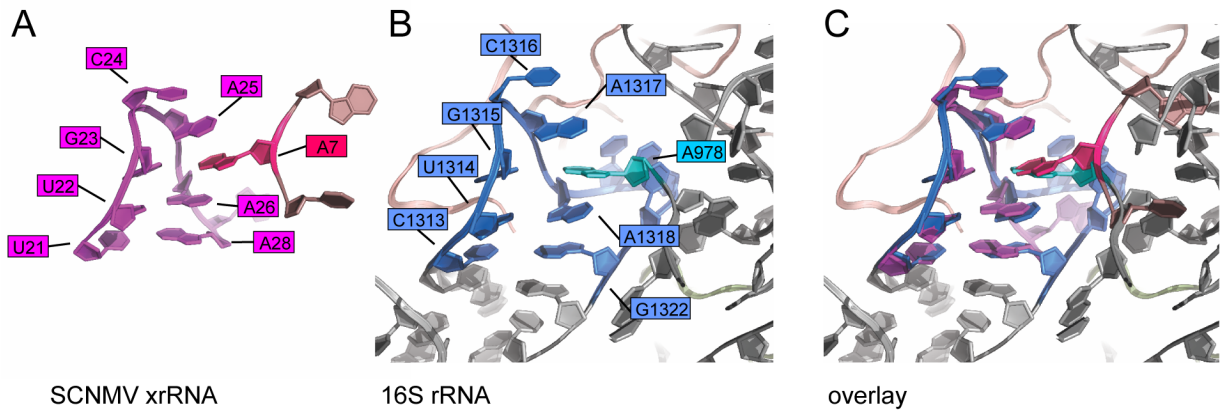

Fig. S7. Similar structures in Dianthovirus xrRNAs and rRNA. (*A*) L2B-A7 interaction of SCNMV xrRNA. Nucleotides forming L2B are shown in magenta, A7 in pink. (*B*) Detail of the 3′ major (3′M) domain of the 16S rRNA from *Thermus thermophilus* (PDB: 4YHH). The nucleotides forming a similar hairpin structure to the SCNMV xrRNA L2B are shown in blue, the docking adenosine is shown in cyan. Numbers according to PDB. (*C*) Alignment of structures from (*A*) and (*B*). RMSD = 0.939 (137 atoms). The similar folds were identified using the substructure search function from DrugSite (https://drugsite.msi.umn.edu/credits).

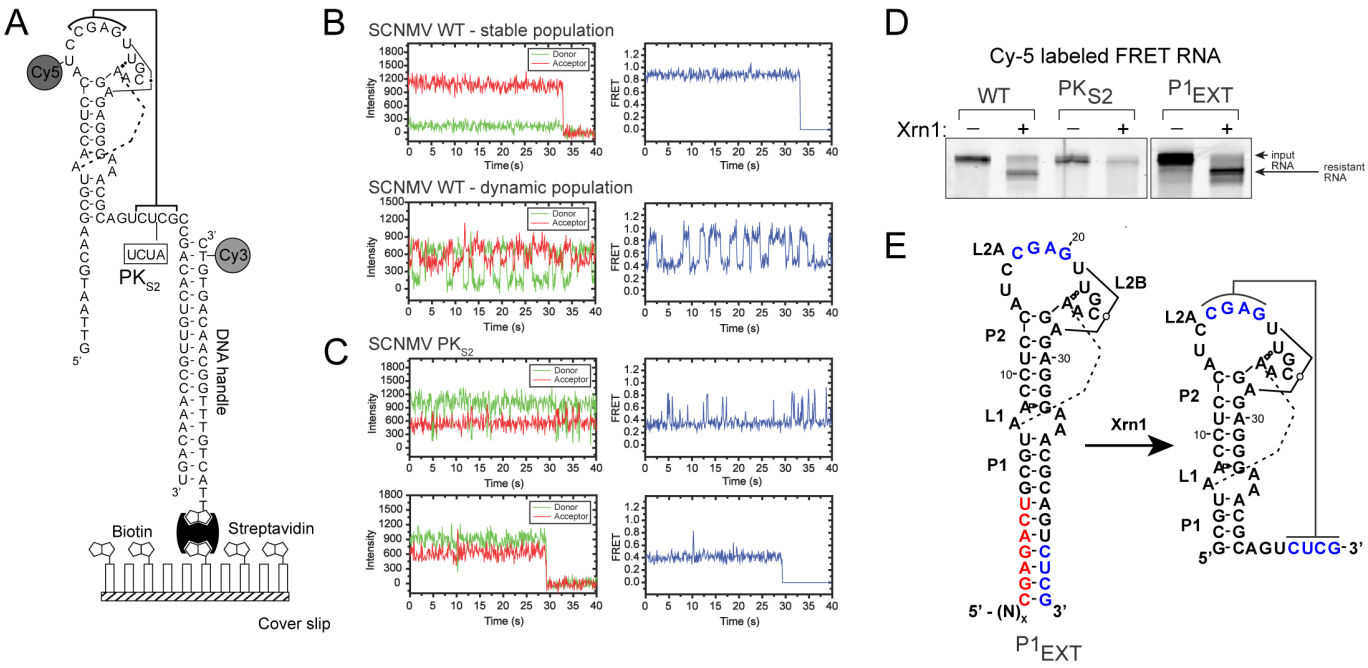

Fig. S8. Structural dynamics of the SCNMV xrRNA. **(***A*) Details of the FRET labeling strategy. Cy5-labeled RNA was annealed to a surface-immobilized, Cy3-labeled DNA oligo. PK_{S2} mutation is shown in the box. A 10-nucleotide leader sequence allowed efficient loading of Xrn1. (*B*) Representative FRET traces of individual SCNMV WT molecules. Top: Stable high-FRET molecule, bottom: dynamic molecule. Total intensities (left) and FRET values (right) are shown. The same molecules are shown in Fig. 4*C*. (*C*) Representative FRET traces of two individual SCNMV PK_{S2} molecules. Total intensities (left) and FRET values (right) are shown. It is less clear if the variations observed between traces (top, bottom) represent a stable and unstable 0.4 FRET state as was observed with the SCNMV WT construct. Importantly, whether or not there are different versions of the 0.4 FRET state has no bearing on the overall interpretation that mutating the pseudoknot heavily favors the 0.4 FRET state. The same molecules are shown in Fig 4*D*. (*D*) *In vitro* Xrn1 degradation assay showing that dye-labeled RNA molecules display the same Xrn1-resistant patterns as unlabeled RNAs. Cy5-labeled RNA was incubated in the presence of recombinant Xrn1, degradation products were resolved by denaturing PAGE and visualized through fluorescence scanning. (*E*) Scheme representing how Xrn1 degradation removes sequence from the 5' end (red) to liberate the base-paired sequence, allowing PK formation. This shifts the SCNMV $P1_{EXT}$ xrRNA molecules from the mid- to high-FRET state. Since the xrRNA requires the pseudoknot in order to resist the activity of Xrn1, the xrRNA must adopt the PK form 'co-degradationally' (i.e. before Xrn1 degrades through nucleotide G3).

Table S1. Data collection and refinement statistics

	Iridium (III) hexamine
Data collection	
Space group	P 61 2 2
Cell dimensions	
a, *b*, *c* (Å)	83.4, 83.4, 94.2
α, β, γ (º)	90, 90, 120
Resolution (Å)	47.10-2.55 (2.66-2.55)*
R_{sym} or R_{merge}	24.1 (156.4)
R_{meas}	24.3 (158.6)
$I/\sigma I$	22.7 (0.9)
CC(1/2)	100 (62.8)
Completeness (%)	99.8 (98.8)
Redundancy	65.1 (22.1)
Refinement	
Resolution (Å)	47.10-2.9
No. reflections	366,075 (33,300)
R_{work} / R_{free}	21.2 (41.7) / 24.9 (52.5)
No. atoms	1044
RNA	946
Ligand/ion	98
B-factors	102.9
RNA	100.8
Ligand/ion	123.6
R.m.s deviations	
Bond lengths (Å)	0.049
Bond angles (º)	1.83

*Highest resolution shell is shown in parenthesis

SI References

1. Chang JH, Xiang S, Xiang K, Manley JL, & Tong L (2011) Structural and biochemical studies of the 5'-->3' exoribonuclease Xrn1. *Nat Struct Mol Biol* 18(3):270-276.
2. Chang JH, *et al.* (2012) Dxo1 is a new type of eukaryotic enzyme with both decapping and 5'-3' exoribonuclease activity. *Nat Struct Mol Biol* 19(10):1011-1017.
3. Mathy N, *et al.* (2007) 5'-to-3' exoribonuclease activity in bacteria: role of RNase J1 in rRNA maturation and 5' stability of mRNA. *Cell* 129(4):681-692.
4. Messing SA, *et al.* (2009) Structure and biological function of the RNA pyrophosphohydrolase BdRppH from Bdellovibrio bacteriovorus. *Structure* 17(3):472-481.
5. Xiong ZG & Lommel SA (1991) Red clover necrotic mosaic virus infectious transcripts synthesized in vitro. *Virology* 182(1):388-392.
6. Webb CH & Luptak A (2011) HDV-like self-cleaving ribozymes. *RNA Biol* 8(5):719-727.
7. Kabsch W (2010) Xds. *Acta Crystallogr D Biol Crystallogr* 66(Pt 2):125-132.
8. Adams PD, *et al.* (2010) PHENIX: a comprehensive Python-based system for macromolecular structure solution. *Acta Crystallogr D Biol Crystallogr* 66(Pt 2):213-221.
9. Emsley P & Cowtan K (2004) Coot: model-building tools for molecular graphics. *Acta Crystallogr D Biol Crystallogr* 60(Pt 12 Pt 1):2126-2132.

10. Emsley P, Lohkamp B, Scott WG, & Cowtan K (2010) Features and development of Coot. *Acta Crystallogr D Biol Crystallogr* 66(Pt 4):486-501.
11. Akiyama BM & Stone MD (2009) Assembly of complex RNAs by splinted ligation. *Methods Enzymol* 469:27-46.
12. Selvin PR & Ha T (2008) *Single-molecule techniques : a laboratory manual* (Cold Spring Harbor Laboratory Press, Cold Spring Harbor, N.Y.) pp vii, 507 p.
1. Chang JH, Xiang S, Xiang K, Manley JL, & Tong L (2011) Structural and biochemical studies of the 5'-->3' exoribonuclease Xrn1. *Nat Struct Mol Biol* 18(3):270-276.
2. Chang JH*, et al.* (2012) Dxo1 is a new type of eukaryotic enzyme with both decapping and 5'-3' exoribonuclease activity. *Nat Struct Mol Biol* 19(10):1011-1017.
3. Mathy N*, et al.* (2007) 5'-to-3' exoribonuclease activity in bacteria: role of RNase J1 in rRNA maturation and 5' stability of mRNA. *Cell* 129(4):681-692.
4. Messing SA*, et al.* (2009) Structure and biological function of the RNA pyrophosphohydrolase BdRppH from Bdellovibrio bacteriovorus. *Structure* 17(3):472-481.
5. Chapman EG, Moon SL, Wilusz J, & Kieft JS (2014) RNA structures that resist degradation by Xrn1 produce a pathogenic Dengue virus RNA. *Elife* 3:e01892.
6. Xiong ZG & Lommel SA (1991) Red clover necrotic mosaic virus infectious transcripts synthesized in vitro. *Virology* 182(1):388-392.
7. Webb CH & Luptak A (2011) HDV-like self-cleaving ribozymes. *RNA Biol* 8(5):719-727.
8. Kabsch W (2010) Xds. *Acta Crystallogr D Biol Crystallogr* 66(Pt 2):125-132.
9. Adams PD*, et al.* (2010) PHENIX: a comprehensive Python-based system for macromolecular structure solution. *Acta Crystallogr D Biol Crystallogr* 66(Pt 2):213-221.
10. Emsley P & Cowtan K (2004) Coot: model-building tools for molecular graphics. *Acta Crystallogr D Biol Crystallogr* 60(Pt 12 Pt 1):2126-2132.
11. Emsley P, Lohkamp B, Scott WG, & Cowtan K (2010) Features and development of Coot. *Acta Crystallogr D Biol Crystallogr* 66(Pt 4):486-501.
12. Akiyama BM & Stone MD (2009) Assembly of complex RNAs by splinted ligation. *Methods Enzymol* 469:27-46.
13. Selvin PR & Ha T (2008) *Single-molecule techniques : a laboratory manual* (Cold Spring Harbor Laboratory Press, Cold Spring Harbor, N.Y.) pp vii, 507 p.